Main Air Pollution Sources Correlated with the Tropospheric NO2 Concentration in Romania as Observed by the Tropospheric Monitoring Instrument (Sentinel-5P)

Kamill Dániel Kovács, Ionel Haidu

How to cite: Kovács, K.D., Haidu, I. (2022) Main Air Pollution Sources Correlated with the Tropospheric No2 Concentration in Romania as Observed by the Tropospheric Monitoring Instrument (Sentinel-5P). *2022 "Air and Water – Components of the Environment" Conference Proceedings*, Cluj-Napoca, Romania, p. 199-216, DOI: 10.24193/AWC2022_19.

MAIN AIR POLLUTION SOURCES CORRELATED WITH THE TROPOSPHERIC NO_2 CONCENTRATION IN ROMANIA AS OBSERVED BY THE TROPOSPHERIC MONITORING INSTRUMENT (SENTINEL-5P)

Kamill Dániel KOVÁCS* [1], Ionel HAIDU [1]

DOI: 10.24193/AWC2022_19

ABSTRACT. Using high-resolution Sentinel-5P satellite data, this study investigates the relationship between the main sources of air pollution and the concentration of NO_2 gas in the tropospheric column during the period 2018-2021 in Romania. NO_2 data, both raster and time series obtained through remote sensing techniques by the TROPOMI sensor were used for this analysis. Kernel density estimation (KDE) was chosen as a technique to determine the magnitude of the spatial densification of the main sources of NO_2 pollution (KDE PS). Hotspot-Coldspot analysis of the NO_2 concentration based on Local Indicators of Spatial Association (LISA) was performed using Getis-Ord Gi* statistic. Besides, a correlation and regression analysis was conducted based on a statistical T-test between KDE PS, elevation above sea level, and mean tropospheric NO_2 concentration during 2018-2021. The results evidenced that traditional air pollution sources continue to determine the NO_2 pollution levels in Romania, these levels aside being also conditioned by the elevation above sea level. We conclude that NO_2 pollution can only be reduced in polluted areas if green energy is favored and measures are taken to mitigate polluting traffic in cities.

Keywords: tropospheric NO_2, Sentinel-5P, air pollution sources, elevation, Romania

1. INTRODUCTION

The aim of the new environmental policies of the European Union is to create healthier living spaces from the local to the country level (European Comission, 2017; Heinelt et al., 2018; Jordan & Adelle, 2012). A key issue in this initiative is air pollution and its anthropogenic sources (Koolen & Rothenberg, 2019; Piotrowicz & Ciaranek, 2014; Suciu et al., 2018). To achieve compliance with the air pollution reduction standards, it is necessary to know not only the magnitude but also the

[1] Université de Lorraine, Laboratoire LOTERR-EA7304, Île du Saulcy, 57045 Metz, France ; Corresponding author, First author : Kamill Dániel Kovács * (email : kamill-daniel.kovacs@univ-lorraine.fr) ; Co-author(s) : Ionel Haidu (email : ionel.haidu@univ-lorraine.fr)

spatial pattern of air pollution at country level and which sources mainly influence the spatiality of the phenomenon.

A group of important gases that can endanger the respiratory health of living beings are NOX, mainly nitric oxide (NO) and nitrogen dioxide (NO_2), although they are essential trace gases in the Earth's atmosphere (Muller, 1992). These gases enter the atmosphere in abundance largely through anthropogenic activities (combustion of fossil fuels, burning of biomass) contributing to the formation of photochemical ozone (smog) and having negative consequences for health (Aggarwal & Toshniwal, 2019; Brewer et al., 1973; Peel et al., 2013).

Several empirical studies addressed the trend of change in the Earth's atmospheric NO_2 concentration with satellite data (Georgoulias et al., 2019; van der A. et al., 2008). These studies consistently found that tropospheric NO_2 generally decreased over the past 2 decades in the developed "western" countries of the world (decrease by ~30%), while it increased considerably in developing regions (in China and India by ~160%, ~33%, respectively).

2. LITERATURE REVIEW

The research literature on Romania combining satellite data with in-situ ground-based measurements started in recent years (Constantin, Voiculescu, et al., 2013; Dragomir et al., 2015; Paraschiv & Paraschiv, 2019; Voiculescu et al., 2020). These studies concluded that tropospheric NO_2 in Romania tended to be higher in cities depending on the course of traffic and daytime and, also, in highly industrialized areas, especially where coal and gas-based industrial or power plants were located. Other researchers measured NO_2 levels with sensor instruments through long pathways in the country and compared the results with satellite data (Constantin, Merlaud, et al., 2013). Furthermore, Paraschiv & Paraschiv (2019) demonstrated that in two Romanian cities, traffic-type sources had a greater contribution to urban pollution than industrial-type sources on a local scale. The variation in near-surface NO_2 concentrations influenced by meteorological parameters was also investigated by implementing in-situ monitoring measurements and comparison with OMI (Ozone Monitoring Instrument) satellite data (Voiculescu et al., 2020). Other researchers focused more on the effects of NO_2 on respiratory health, among other ambient air pollutants (Leitte et al., 2009). More recently, the effect of COVID-19 lockdown on NO_2 levels was studied in a Romanian city (Roșu et al., 2021).

Even though these studies focused on urban areas or specific pathways in Romania, insufficient attention has been paid to what correlation exists between the main sources of pollution responsible for NO_2 emission and the spatio-temporal pattern of tropospheric NO_2 concentration at the country level. Furthermore, NO_2 is generally assumed to be dependent on anthropogenic and meteorological factors. However, this paper suggests that it is also conditioned by an independent variable on a small geographic scale.

In the context of the air pollution sources in Romania, this study addresses the concentration of NO_2 gas in the tropospheric column over the territory of the country with high spatial resolution satellite data (approx. 1113.2 m) acquired from the TROPOMI sensor of the Sentinel-5P mission. The research hypothesis of the study was that the main sources of air pollution in Romania (i.e. coal and gas power plants, chemical and steel industrial plants, and urban population size of cities) are significantly influencing the levels of near-surface NO_2.

3. DATA AND SOFTWARE USED

The NO_2 data used comes from the Copernicus database (ESA, n.d.). Point data of the electrical and industrial plants were obtained from the Global Power Plant Database (World Resources Institute, n.d.). Additionally, an SRTM digital elevation model (DEM) was used for subsequent analysis regarding the country's territory. The spatial analyzes were conducted with QGIS, SAGA GIS, and R open-source software.

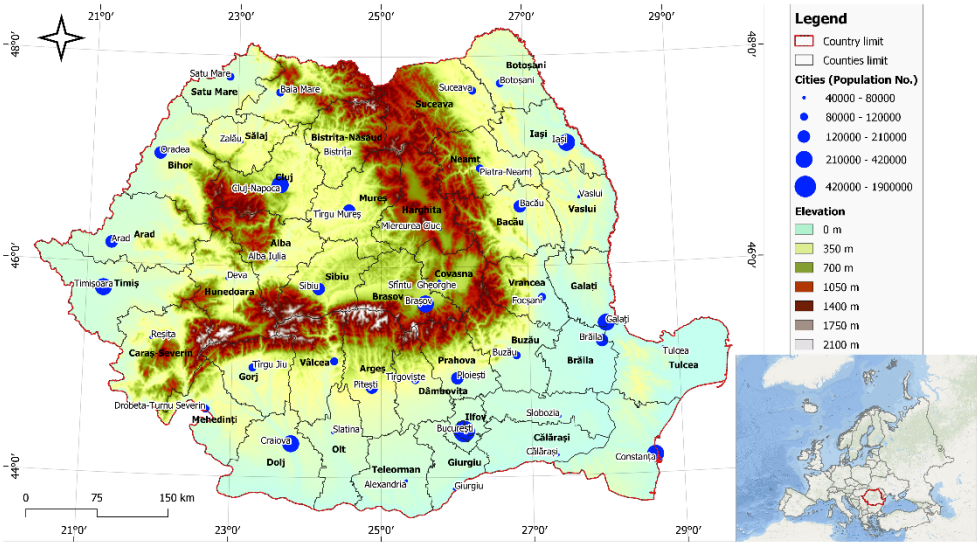

Fig. 1. ***Location of Romania and its general characterization***

4. METHODS

4.1. Obtaining the tropospheric NO_2 data

Tropospheric column NO_2 data was retrieved from satellite measurements made by the TROPOMI sensor of the Sentinel-5P satellite between 2018-2021 over the entire territory of Romania (Fig. 1). These data were obtained through Google Earth Engine (GEE) platform by means of code, creating a filter for the region of interest and the analysis period (Kovács, 2021). The 'Offline' (OFFL) satellite data product was used because OFFL products are generally considered better in terms of quality than the

'Near Real Time' (NRTI) products, although research indicates that there are slight accuracy differences between the two satellite products (Verhoelst et al., 2021).

The code first called the corresponding database and then the data was transformed from Level 2 (L2) to Level 3 (L3). The conversion to L3 was performed with the *harpconvert* tool by executing the *bin_spatial* operation. In the second step, the data was filtered to remove pixels that had less than 75% quality control values in the NO_2 tropospheric density band. In the third step, after generating the tropospheric NO_2 density image, the raster image containing the NO_2 amount information was exported in gridded data format. This result was incorporated into a GIS environment for subsequent analysis.

4.2. Estimation of the spatial density of main NO_2 sources with Kernel method

Based on long-term TROPOMI observations, the main sources of NO_2 determined in this analysis were power plants (coal and gas types), industrial plants (chemical and steel types) in operation over the national territory and abroad the boundaries of the country within a radius of 100 km and, in addition, the main cities of the country were considered based on rank and population.

The spatial density of the determined NO_2 sources was performed with the Kernel Density Estimation (KDE) method, resulting in a practical application of the theoretical kernel function: the estimation of the spatial density of the main polluting sources (KDE PS). KDE for entry points calculates the surface density of features around raster cells. Theoretically, a smoothly curved surface fits over each point entered in the calculation equation. The value of this resulting surface is highest at the exact location of the point and decreases as the distance from the points increases (ArcGIS, n.d.). The mathematical function is based on the quartic function described by Silverman (1986) (1):

$$\widehat{p_n}(x) = \frac{1}{nh}\sum_{i=1}^{n} K\left(\frac{x_i - x}{h}\right) \quad (1)$$

where $K(x)$ is the kernel function with Gaussian distribution and $h > 0$ is the bandwidth controlling the magnitude of the smoothing. The KDE function smooths each data point xi into small protuberances and aggregates all of them to get the final estimated density.

Based on this function, the predicted density at a new different location on the surface (x, y) is calculated as follows (ArcGIS, n.d.) (2):

$$KDE\ PS = \frac{1}{(radius)^2}\sum_{i=1}^{n}\left[\frac{3}{\pi} * pop_i\left(1 - \left(\frac{dist_i}{radius}\right)^2\right)^2\right] \quad (2)$$

for $dist(i) < radius$, where $i = 1, \ldots, n$ are the points entered into the analysis, $pop(i)$ is the weight value and $dist(i)$ denotes the distance between point i and the new location.

KDE was performed with a SAGA GIS tool: 'Kernel Density Estimation'. This algorithm required the analyzed entry points (NO_2 sources), the size of the search

radius, and the weight for the points xi, …, n. The search radius was calculated as follows (Fotheringham et al., 2000) (3):

$$h_{opt} = \left(\frac{2}{3n}\right)^{\frac{1}{4}} \sigma \quad (3)$$

where σ denotes the standard distance and n is the number of observed points.
σ and the mean center were calculated with the 'Spatial point pattern analysis' QGIS tool. For the "weight" field, to each xi element was assigned the value 1 because each point had the same importance in the KDE. According to this, the calculation equation is (ArcGIS, n.d.) (4):

$$SD_w = \sqrt{\frac{\sum_{i=1}^{n} w_i (x_i - \bar{X}_w)^2}{\sum_{i=1}^{n} w_i} + \frac{\sum_{i=1}^{n} w_i (y_i - \bar{Y}_w)^2}{\sum_{i=1}^{n} w_i} + \frac{\sum_{i=1}^{n} w_i (z_i - \bar{Z}_w)^2}{\sum_{i=1}^{n} w_i}} \quad (4)$$

where SD_w denotes the weighted standard distance with a designated weight, x_i, y_i, z_i are the coordinates of point *i*, w_i is the weight for point *i*, and $\{\bar{X}_w, \bar{Y}_w, \bar{Z}_w\}$ represent the weighted mean center. The KDE output is a continuous surface raster.

4.3. Determination of significant correlation between variables

The statistical significance of the correlation between the investigated variables was tested using the T-test ($t_{r_{xy}}$) and by evidencing the coefficient of determination (r_{xy}^2). The T-test reveals whether a correlation between variables is significantly different from 0 or not. If different, it can be affirmed with statistical evidence that there is a strong interdependence between the variables. The null hypothesis (H0) of the T-test states that $\rho = 0$, which indicates that there is no significant relationship between X and Y. As an alternative to this, hypothesis 1 (H1) states that $\rho \neq 0$, which concludes a significant relationship and interdependence between X and Y in an f(x) function. The T-test calculation is widely known (Kanji, 2006) (5):

$$t_{r_{xy}} = \frac{r_{xy}\sqrt{n-2}}{\sqrt{1-r_{xy}^2}} \quad (5)$$

$t_{r_{xy}}$ has a Student t distribution with *n - 2* degrees of freedom. r_{xy} is the correlation coefficient, r_{xy}^2 is the coefficient of determination, and n is the number of pair observations. If the test result is $t_{r_{xy}} \leq CV$, H0 is accepted or, alternatively, if $t_{r_{xy}} > CV$, H0 is rejected by opting for H1. Expressing the same on p-values, H0 is maintained if $p > 0.05$, and H1 is adopted if $p < 0.05$ (at significance level $\alpha = 0.05$).

4.4. Hotspot–Coldspot analysis of NO_2 concentration with Local Getis-Ord GI*

The combination of the Local Getis-Ord GI* statistic's results determines the spatial clustering of a studied phenomenon. The hotspot–coldspot analysis was performed to determine the clustering phenomenon of tropospheric NO_2 concentration during 2018-2021. The contribution of the hotspot–coldspot analysis is that a single observed high or low value of NO_2 concentration cannot be evaluated

as a statistically significant and consistent spatial cluster over time. To be considered a 'hotspot' cluster, a high value must be surrounded by other similar high values, and likewise, for 'coldspot', a low value must be surrounded by other low values in the spatial proximity of the NO_2 values (Getis & Ord, 1992; Ord & Getis, 1995).

The value of the GI* statistic is traditionally calculated as (Ord & Getis, 1995) (6):

$$G_i^* = \frac{\sum_{j=1}^{n} w_{i,j}x_j - \bar{X}\sum_{j=1}^{n} w_{i,j}}{S\sqrt{\frac{\left[n\sum_{j=1}^{n} w_{i,j}^2 - \left(\sum_{j=1}^{n} w_{i,j}\right)^2\right]}{n-1}}} \quad (6)$$

$x(j)$ denotes the attribute value of the spatial feature j, $w(i, j)$ is a given spatial weight between features i and j, n is the total number of spatial features with which the analysis is conducted, and, accordingly $\bar{X}$ and S are the mean and variance components of the sample, respectively (7(8):

$$\bar{X} = \frac{\sum_{j=1}^{n} x_j}{n} \quad (7)$$

$$S = \sqrt{\frac{\sum_{j=1}^{n} x_j^2}{n} - (\bar{X})^2} \quad (8)$$

The hotspot–coldspot analysis with Local Getis-Ord GI* was conducted in a GIS interface using the 'Hotspot Analysis' plug-in. This vector analysis plug-in was detailed and implemented by several researchers (Guerri et al., 2021; D. Oxoli et al., 2017; Daniele Oxoli et al., 2018). The GI* z-score result indicates the intensity of the clustering. A high positive z-score indicates that the high NO_2 concentration values are forming hotspots, and conversely, a high negative z-score indicates that the low NO_2 concentration values are clustering as coldspots. In the other part of the GI*, the resulting p-value indicates probability. A very small resulting p-value means that the observed spatial pattern is unlikely to be the result of a random process and, consequently, H0 is rejected (i.e. randomness).

The spatial features involved in the analysis were the communes of Romania that represent the base territorial units of the country. By performing zonal statistics, the median value of the raster image was obtained, which represented the NO_2 concentration of the tropospheric column in each of the communes. The hotspot–coldspot analysis was accomplished with these data extracted at the communes' level.

4.5. Sampling between hotspots–coldspots, elevation, and KDE PS values

Representative sampling between NO_2 hotspots–coldspots, elevation, and KDE PS values was completed in five steps: (1) assignment of the values 3 to -3 in the attribute table for the significant hotspots–coldspots, according to the confidence levels based on the relation between z-score and p-value (Table 1); (2) rasterization process of the reclassification with the 'Rasterize (vector to raster)' QGIS tool; (3) extraction of the significant clusters with the raster calculator using the logical expression (9):

$$("HC" != 0) * "HC" / ("HC" != 0) * 1 + ("HC" = 0) * 0 \quad (9)$$

where HC is the hotspot–coldspot raster.

And ultimately, the last stages: (4) generation of random points within the limits of the extracted raster layer, according to a significant sample size calculated with the Sample Size Calculator available on the internet (SurveyMonkey, n.d.) and (5) point sampling on the raster layers (hotspots–coldspots extracted, elevation, and KDE PS).

Table 1. ***Logical relationship between z-score and p-value for the confidence levels in the hotspot–coldspot analysis and its reclassification***

Z-score and p-value Relation	Confidence Level	Reclassification Value
"Z-score" <= -2.58 AND "p-value" <= 0.01	Coldspot 99%	-3
"Z-score" <= -1.96 AND "Z-score" > -2.58 AND "p-value" <= 0.05 AND "p-value" > 0.01	Coldspot 95%	-2
"Z-score" <= -1.65 AND "Z-score" > -1.96 AND "p-value" <= 0.1 AND "p-value" > 0.05	Coldspot 90%	-1
"Z-score" > -1.65 AND "Z-score" < 1.65 AND "p-value" > 0.1	Not Significant/Random	0
"Z-score" >= 1.65 AND "Z-score" < 1.96 AND "p-value" <= 0.1 AND "p-value" > 0.05	Hotspot 90%	1
"Z-score" >= 1.96 AND "Z-score" < 2.58 AND "p-value" <= 0.05 AND "p-value" > 0.01	Hotspot 95%	2
"Z-score" >= 2.58 AND "p-value" <= 0.01	Hotspot 99%	3

4.6. Trend identification in the tropospheric NO_2 time series over 35 cities and NO_2 forecast

The mean tropospheric NO_2 time series data over 35 Romanian cities were obtained from the Sentinel-5P COPERNICUS/S5P/OFFL/L3_NO_2 database and generated using GEE code (Kovács, 2021). The subsequent analysis of the time series was performed using R software packages (‘tseries’, ‘seasonal’, ‘forecast’, ‘ggplot2’, ‘openxlsx’). The forecast of tropospheric NO_2 concentration over 35 cities was realized with an ARIMA model using the auto.arima tool of R’s ‘forecast’ library.

5. RESULTS

The results of obtaining tropospheric NO_2 data captured by the TROPOMI sensor onboard the Sentinel-5P satellite revealed the average NO_2 concentration in Romania between 2018-2021 (Fig. 2). Fig. 2 also presents the main power and industrial plants in the country and, besides, the cities classified by population size according to census data. On the map, two main spots of high NO_2 concentrations were observed: on the middle course of the Jiu River in the proximity of coal deposits (Rovinari,

Turceni, Işalnița, and CE Craiova energy complex) (Gorj, Dolj counties) and around the city of Bucharest. Other locations of high concentration appeared around several cities and, also, along the communication lines by road (high concentrations in form of continuous lines) or in depressions (Culoarul Orăștiei, Culoarul Alba Iulia-Turda, Depresiunea Brașovului). In general, this result evidenced a relatively higher concentration over extensive plains, depressions, and main valleys than in mountainous areas of the country's territory. However, exceptions to this pattern were also found (such as the Danube Delta). From a broad perspective, the average tropospheric NO_2 concentration between 2018-2021 was well reflected by the three main sources of air pollution: industrial plants, power plants, and major cities.

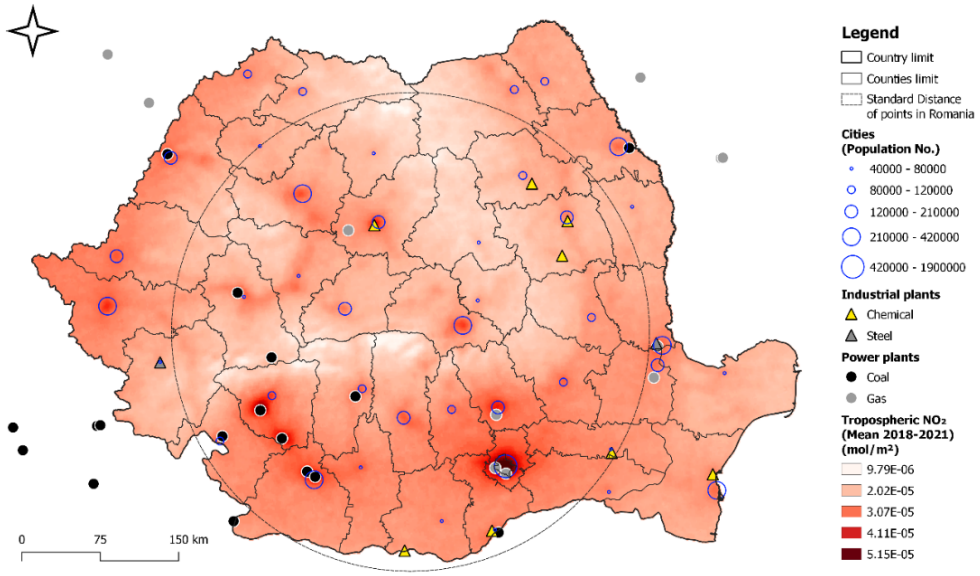

Fig. 2. ***Average tropospheric NO_2 concentration between 2018-2021 and the main sources of air pollution***

The result of the spatial density estimation of NO_2 sources (KDE PS) revealed the areas which have the highest energy and industrial productivity of the country, by also considering the population size of the cities (Fig. 3). This result evidenced six major PS densifications with their ramifications: the area of the capital Bucharest (Ilfov, Prahova, Giurgiu counties), the area of the Jiu valley in its middle course (Târgu Jiu-Craiova) (Gorj, Dolj counties), the Galati-Braila axis on the banks of the Danube (Galați, Brăila counties), the Moldovan center (Neamț, Bacău counties), the Transylvanian center (the Mureș, Cluj counties), and western areas (Bihor, Arad, Timiș counties) mainly related to the western cities of Romania. The result of the KDE PS estimation also considered NO_2 sources outside the country's borders within a radius of 100 km, because these sources can have an impact on the country's territory due to atmospheric circulation.

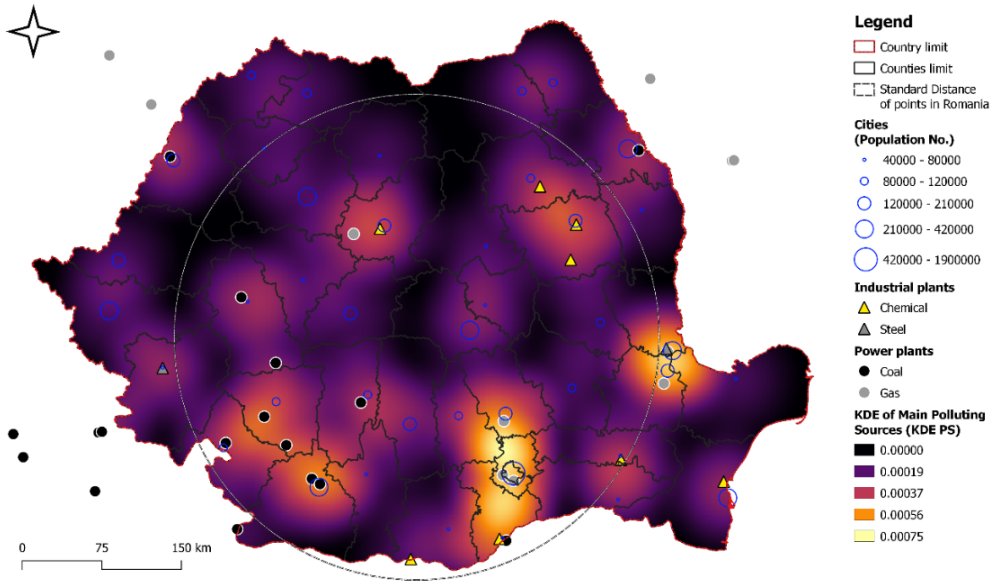

Fig. 3. ***KDE of the main air pollution sources (KDE PS)***

The result of the correlation analysis between the mean tropospheric NO_2 concentration (2018-2021) and KDE PS revealed that there was a strong direct and statistically significant connection between these variables in the counties of Romania (Table 2, Fig. 4). The correlation coefficient between the variables was r = 0.796. Further, the coefficient of determination using a linear curve was $r^2 = 0.633$, while a polynomial curve of degree 2 better described the points: $r^2 = 0.726$. The result of the T-test for correlation ($t_{r_{xy}}$) concluded that there was a statistically significant correlation between the KDE of the main pollution sources and the mean tropospheric NO_2 concentration between the period 2018-2021 ($t_{r_{xy}} = 3.716, CV = 2.021, p < 0.05$). This means that as the density of polluting sources increased, the concentration of near-surface NO_2 levels also increased.

Table 2. ***Results of the T-test for correlation***

Variables	r_{xy}	r^2_{xy}	*Two-tailed T-test statement*	*CV*	*p-value (<0.05)*	*Conclusion*
KDE PS & NO_2	0.796	0.633	t(40) = 3.716, α=0.05	2.021	0.001	H1: ρ≠0

The hotspot–coldspot analysis with Local Getis-Ord GI* brought valuable results for the definitive identification under statistical consistency of the areas with the highest (hotspots) and lowest (coldspots) concentration of tropospheric NO_2 between 2018-2021 (Fig. 5). Three large hotspots were detected (Bucharest area, Central Jiu Valley area, Arad-Timişoara area), among other four medium hotspots (areas of Oradea, Galați, Târgu Mureş, and Cluj-Napoca) and three minor hotspots (areas

around Brașov, Vâlcea, and Deva). The coldspots corresponded mainly to mountainous and/or sparsely populated areas (Danube Delta region).

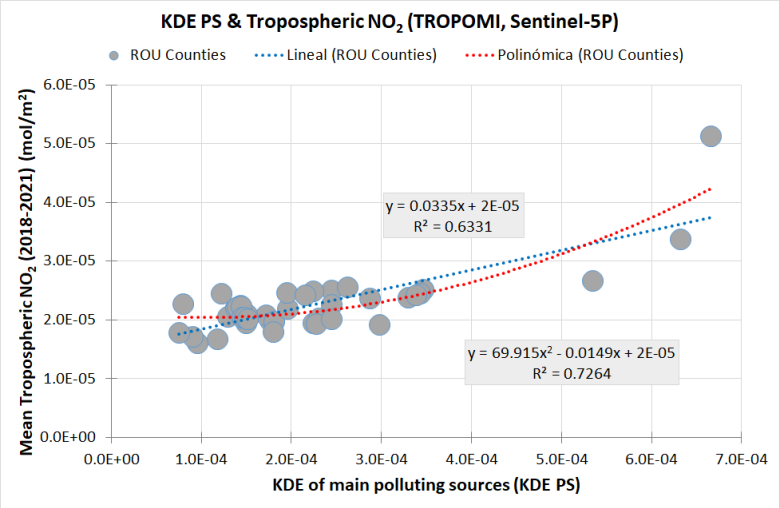

Fig. 4. ***Correlation between KDE PS and mean tropospheric NO_2 concentration in the counties***

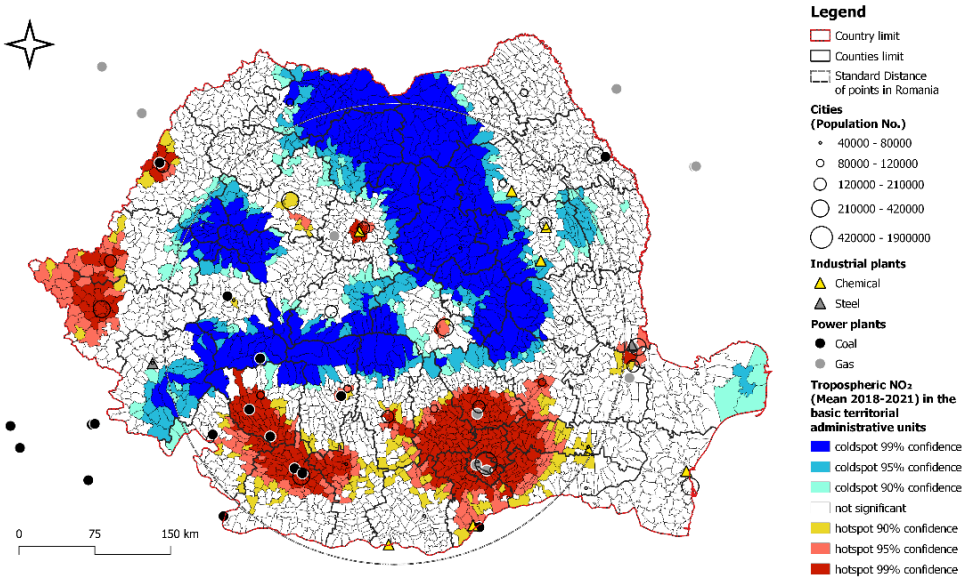

Fig. 5. ***Significant hotspots and coldspots of tropospheric NO_2 concentration between 2018-2021***

The result of representative sampling between hotspots–coldspots and elevation values above sea level revealed that significant NO_2 hotspots tended to be

concentrated between 0 and 500 m altitude, while most NO_2 coldspots occurred above 500 m (Fig. 6). This fact demonstrates the dependence of NO_2 concentration levels on altitude above sea level ($r^2 = 0.66$) (Fig. 7).

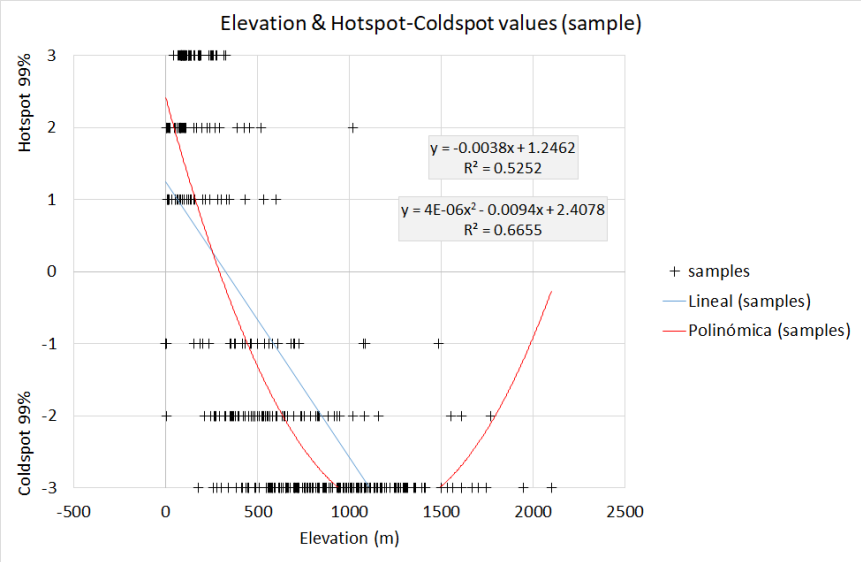

Fig. 6. ***Relationship between elevation above sea level and NO_2 hotspots-coldspots***

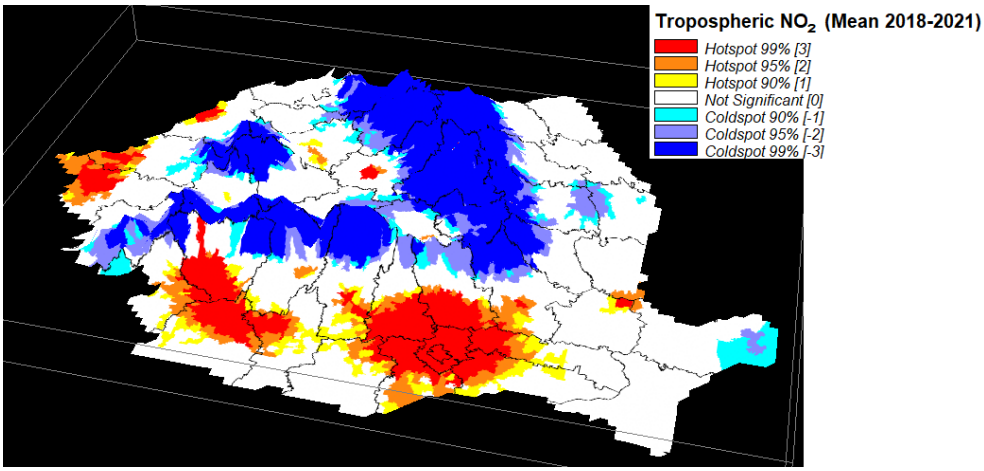

Fig. 7. ***3D representation of NO_2 hotspots-coldspots on the digital elevation model of Romania***

Moreover, the sampling analysis between the hotspots–coldspots and KDE PS values demonstrated that the NO_2 hotspots tended to appear in areas with a higher density of polluting sources, while the NO_2 coldspots occurred with an inclination towards the low KDE PS values (Fig. 8). This behavior evidenced the determining

spatial relationship between the NO_2 clustering phenomenon and the densification of polluting sources in Romania.

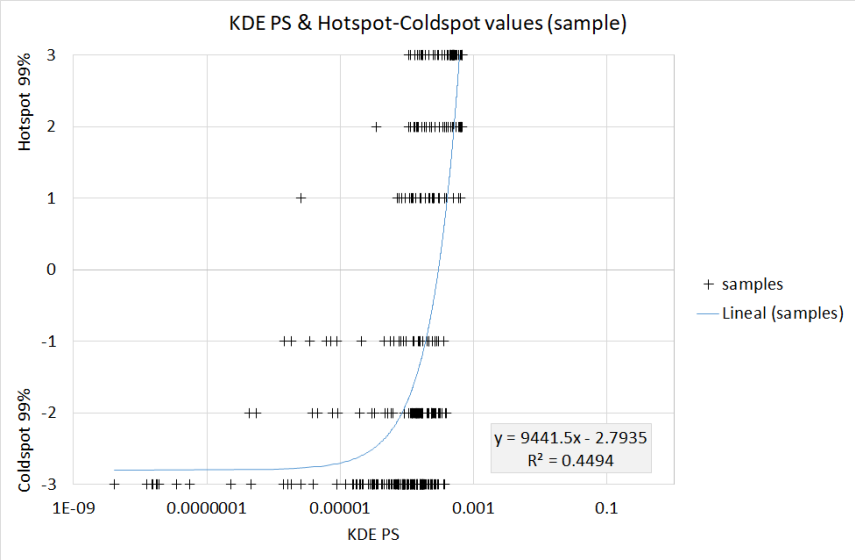

Fig. 8. ***Relationship between KDE PS and NO_2 hotspots-coldspots***

With zonal statistical analysis, the average NO_2 concentration was evidenced during 2018-2021 in 35 Romanian cities (Fig. 9). This result indicated that the five most polluted urban areas in terms of near-surface NO_2 are: Bucharest (51.3 µmol/m^2), Craiova (37.2 µmol/m^2), Ploiești (35.1 µmol/m^2), Târgu Mureș (33.1 µmol/m^2), and Timișoara (31.84 µmol/m^2).

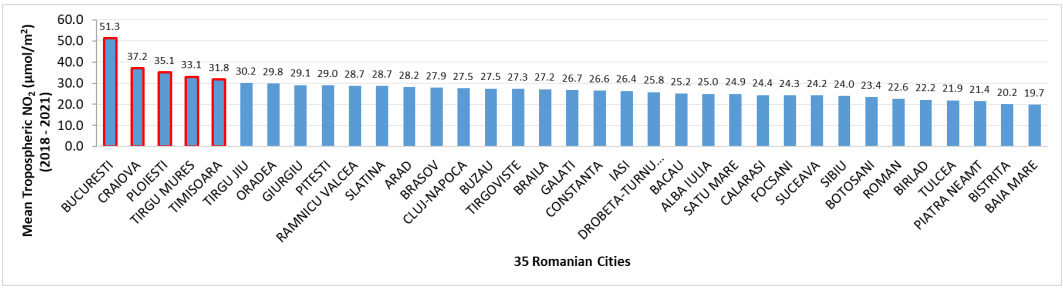

Fig. 9. ***Mean tropospheric NO_2 concentration during 2018-2021 in 35 Romanian urban areas***

The average NO_2 tropospheric time-series data for 35 Romanian cities between the period 2018-2021 explained that there was a cyclical pattern in the behavior of the near-surface NO_2 concentration (Fig. 10, Fig. 11). During the winter-spring, higher levels of NO_2 used to occur than during summer. The result of the time series decomposition showed that there was a strong seasonal component in the data (Fig. 10). Seasonality was also demonstrated to be present in the data by the Augmented

Dickey-Fuller Test (Dickey-Fuller = -4.8454, Lag order = 3, p-value < 0.01). Furthermore, this result revealed that from the second half of 2020 there was a notable increase trend in all 35 cities in the country (Fig. 10).

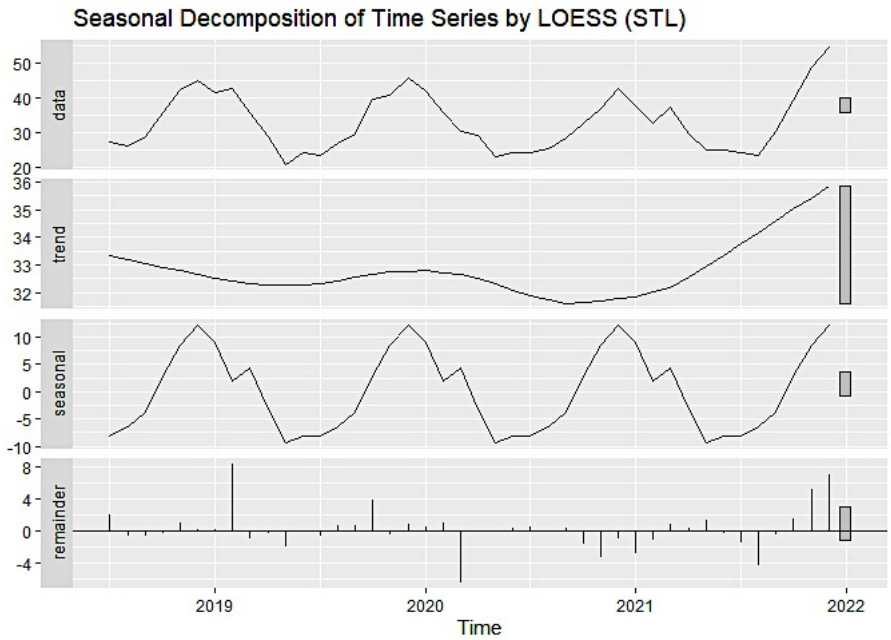

Fig. 10. ***LOESS (STL) decomposition of the tropospheric NO_2 time series in 35 cities***

Based on the detected autocorrelation and stationarity, the seasonal adjustment of the time series allowed obtaining the forecast results from an ARIMA(2,0,1)(1,0,0)[12] model that best described the components of the time series (Table 3). The result of the forecast indicated that the strong seasonal pattern would continue in the coming years, however, with a slightly increasing trend of the average and upper forecast values (Fig. 11). Despite this, the upward trend observed may have been circumstantial due to the resumption of industrial and transportation activity following the relief from anti-COVID-19 measures.

Table 3. ***Details and specifications of the implemented ARIMA(2,0,1)(1,0,0)[12] model***

Coefficients:	ar1	ar2	ma1	sar1	mean	
	1.6442	-0.9038	-0.7637	0.3098	32.766	
s.e.	0.0900	0.0782	0.1707	0.2320	0.704	
sigma^2 estimated as 11.34: log likelihood=-110.41						
AIC=232.82 AICc=235.22 BIC=243.25						
Training set error measures:						
ME	RMSE	MAE	MPE	MAPE	MASE	ACF1
0.03151248	3.16096	2.663424	-1.03175	8.149927	0.8447849	-0.05477575

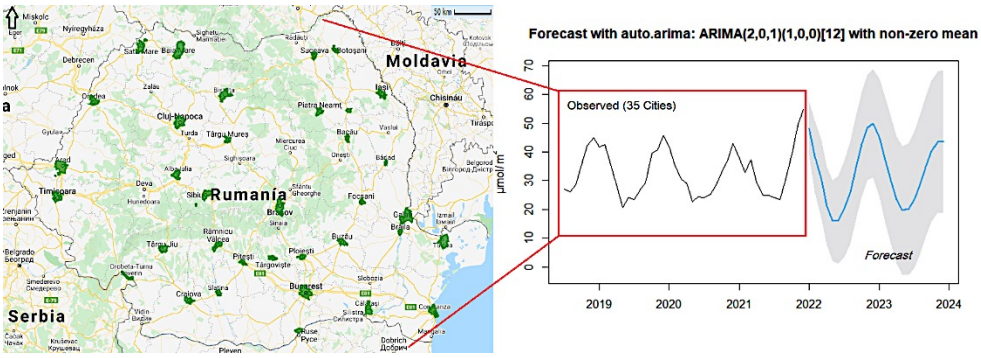

Fig. 11. ***Average concentration of tropospheric NO_2 in 35 cities between 2018-2021 and its forecast***

6. DISCUSSIONS

The research problem of this study was whether or not pollution sources such as traditional coal- and gas-based power industry, chemical and steel industry, and city-related human impact are still determining the concentration of NO_2 gas in the tropospheric column. This study demonstrates a strong correlation between these sources and recent NO_2 levels (2018-2021) over the entire territory of Romania. It has also been shown that NO_2 in 35 Romanian cities has a cyclical behavior over the years with an increasing trend that would tend to increment continuously in the future. Furthermore, this analysis supports the theory that high and low NO_2 concentrations are also conditioned by elevation.

In line with the hypothesis, the TROPOMI data recorded between 2018-2021 confirm that the main traditional sources of pollution continue to significantly influence NO_2 levels in Romania today, as indicated by research in the past (Constantin, Voiculescu, et al., 2013; Dragomir et al., 2015; Paraschiv & Paraschiv, 2019; Voiculescu et al., 2020). In addition, compared with the discoveries of Constantin, Voiculescu, et al., (2013), it was seen that new spots of high NO_2 concentration appeared after the period 1996-2010.

The results of this study contribute to a clearer understanding of the relationship between pollution sources and the spatial pattern of NO_2 concentration at the country level. While previous research has focused on monitoring specific areas or pathways (Constantin, Merlaud, et al., 2013; Paraschiv & Paraschiv, 2019; Voiculescu et al., 2020; Roşu et al., 2021), these results demonstrate that NO_2 levels throughout the country still depend on traditional sources that should be minimized according to the EU's environmental policy. Compared to the research conducted by Roşu et al. (2021), this study indicates that at the level of 35 cities in an ensemble, no evident NO_2 reduction was observed due to anti-COVID-19 measures, however, from the second half of 2020, an increasing trend was detected.

It is beyond the scope of this study to address the issue of validating TROPOMI satellite observations with in-situ ground monitoring data for the entire territory of

Romania. However, high-resolution satellite data reveals the current main spots of air pollution in Romania correlated with the sources that best explain it. Further research is needed to validate the Sentinel-5P data with ground-based data in various areas of Romania.

CONCLUSIONS

This research aimed to identify the areas with the highest prevalent near-surface concentration of NO_2 over the recent years in Romania and, conjointly, to indicate the main poles of the air pollution sources. The findings proved that there were a strong and statistically significant linkage between these main air polluting sources in the country, elevation above sea level, and the space-time concentration levels of NO_2.

The results suggest that the reduction of near-surface NO_2 concentration in Romania could only be achieved if the energy industry is restructured as soon as possible in favor of green energy production and measures to restrict polluting traffic are implemented in cities.

REFERENCES

1. Aggarwal, A., & Toshniwal, D. (2019). Detection of anomalous nitrogen dioxide (NO_2) concentration in urban air of India using proximity and clustering methods. *Journal of the Air & Waste Management Association*, *69*(7), 805–822. https://doi.org/10.1080/10962247.2019.1577314
2. ArcGIS. (n.d.). *How Kernel Density works—ArcGIS Pro | Documentation*. Retrieved July 27, 2021, from https://pro.arcgis.com/en/pro-app/latest/tool-reference/spatial-analyst/how-kernel-density-works.htm.
3. Brewer, A. W., Mcelroy, C. T., & Kerr, J. B. (1973). Nitrogen dioxide concentrations in the atmosphere. *Nature*, *246*(5429), 129–133. https://doi.org/10.1038/246129a0
4. Constantin, D. E., Merlaud, A., Roozendael, M. Van, Voiculescu, M., Fayt, C., Hendrick, F., Pinardi, G., & Georgescu, L. (2013). Measurements of Tropospheric NO_2 in Romania Using a Zenith-Sky Mobile DOAS System and Comparisons with Satellite Observations. *Sensors 2013, Vol. 13, Pages 3922-3940*, *13*(3), 3922–3940. https://doi.org/10.3390/S130303922
5. Constantin, D. E., Voiculescu, M., & Georgescu, L. (2013). Satellite observations of NOtrend over Romania. *The Scientific World Journal*, *2013*. https://doi.org/10.1155/2013/261634
6. Dragomir, C. M., Constantin, D. E., Voiculescu, M., Georgescu, L. P., Merlaud, A., & Van Roozendael, M. (2015). Modeling results of atmospheric dispersion of NO_2 in an urban area using METI–LIS and comparison with coincident mobile DOAS measurements. *Atmospheric Pollution Research*, *6*(3), 503–510. https://doi.org/10.5094/APR.2015.056
7. ESA. (n.d.). *Copernicus Open Access Hub*. Retrieved January 12, 2022, from https://scihub.copernicus.eu/
8. European Comission. (2017). *Special Eurobarometer 468: Attitudes of European citizens towards the environment - Datasets*. https://data.europa.eu/euodp/en/data/dataset/S2156_88_1_468_ENG. Accessed on 10

January 2022.
9. Fotheringham, A. S., Brunsdon, C., & Charlton, M. (2000). *Quantitative Geography : Perspectives on Spatial Data Analysis.* Sage Publications. https://books.google.com/books/about/Quantitative_Geography.html?hl=es&id=1uVOAAAAMAAJ
10. Georgoulias, A. K., Van Der, R. A. J., Stammes, P., Folkert Boersma, K., & Eskes, H. J. (2019). Trends and trend reversal detection in 2 decades of tropospheric NO_2 satellite observations. *Atmospheric Chemistry and Physics*, *19*(9), 6269–6294. https://doi.org/10.5194/ACP-19-6269-2019
11. Getis, A., & Ord, J. K. (1992). The Analysis of Spatial Association by Use of Distance Statistics. *Geographical Analysis*, *24*(3), 189–206. https://doi.org/10.1111/J.1538-4632.1992.TB00261.X/ABSTRACT
12. Guerri, G., Crisci, A., Messeri, A., Congedo, L., Munafò, M., & Morabito, M. (2021). Thermal Summer Diurnal Hot-Spot Analysis: The Role of Local Urban Features Layers. *Remote Sensing 2021, Vol. 13, Page 538*, *13*(3), 538. https://doi.org/10.3390/RS13030538
13. Heinelt, H., Malek, T., Smith, R., & Toller, A. E. (2018). European union environment policy and new forms of governance: A study of the implementation of the environmental impact assessment directive and the eco-management and audit scheme regulation in three member states. In H. Heinelt (Ed.), *European Union Environment Policy and New Forms of Governance: A Study of the Implementation of the Environmental Impact Assessment Directive and the Eco-management and Audit Scheme Regulation in Three Member States: A Study of the Implementation of the E* (1st Editio). Taylor and Francis Inc. https://doi.org/10.4324/9781315202730
14. Jordan, A., & Adelle, C. (2012). Environmental policy in the EU. In A. Jordan & C. Adelle (Eds.), *Environmental Policy in the EU: Actors, Institutions and Processes, Third Edition* (3rd ed.). Taylor and Francis. https://doi.org/10.4324/9780203109823
15. Kanji, G. K. (2006). t-test of a correlation coefficient. In *100 Statistical Tests* (3rd ed., p. 39). The Cromwell Press Ltd. https://www.researchgate.net/profile/Paul-Louangrath/post/Ranking_or_scoring_variables_using_conditional_probability/attachment/59d63c45c49f478072ea7c1a/AS%3A273748962283533%401442278246675/download/100+Statistical+Tests.pdf. Accessed on January 10, 2022.
16. Koolen, C. D., & Rothenberg, G. (2019). Air Pollution in Europe. *Chemsuschem*, *12*(1), 164. https://doi.org/10.1002/CSSC.201802292
17. Kovács, K. D. (2021). *S5P Atmospheric Analysis: Grand Est - Earth Engine Code Editor*. Google Earth Engine. https://code.earthengine.google.com/e867da312ae1b543798e17e8eb6a78ed?noload=true. Accessed on January 10, 2022.
18. Leitte, A. M., Petrescu, C., Franck, U., Richter, M., Suciu, O., Ionovici, R., Herbarth, O., & Schlink, U. (2009). Respiratory health, effects of ambient air pollution and its modification by air humidity in Drobeta-Turnu Severin, Romania. *Science of The Total Environment*, *407*(13), 4004–4011. https://doi.org/10.1016/J.SCITOTENV.2009.02.042
19. Muller, J. F. (1992). Geographical distribution and seasonal variation of surface emissions and deposition velocities of atmospheric trace gases. *Journal of Geophysical Research: Atmospheres*, *97*(D4), 3787–3804. https://doi.org/10.1029/91JD02757
20. Ord, J. K., & Getis, A. (1995). Local Spatial Autocorrelation Statistics: Distributional Issues and an Application. *Geographical Analysis*, *27*(4), 286–306.

https://doi.org/10.1111/j.1538-4632.1995.tb00912.x
21. Oxoli, D., Prestifilippo, G., Bertocchi, D., & Zurbarán, M. (2017). Enabling spatial autocorrelation mapping in QGIS: The Hotspot Analysis Plugin. *Geoingegneria Ambientale e Mineraria*, *151*(2), 45–50. https://www.researchgate.net/publication/322357329_Enabling_spatial_autocorrelation_mapping_in_QGIS_The_hotspot_analysis_plugin. Accessed on 10 January 2022.
22. Oxoli, Daniele, Molinari, M. E., & Brovelli, M. A. (2018). Hotspot analysis, an open source GIS tool for exploratory spatial data analysis: Application to the study of soil consumption in Italy. *Rendiconti Online Societa Geologica Italiana*, *46*, 82–87. https://doi.org/10.3301/ROL.2018.56
23. Paraschiv, S., & Paraschiv, L. S. (2019). Analysis of traffic and industrial source contributions to ambient air pollution with nitrogen dioxide in two urban areas in Romania. *Energy Procedia*, *157*, 1553–1560. https://doi.org/10.1016/J.EGYPRO.2018.11.321
24. Peel, J. L., Haeuber, R., Garcia, V., Russell, A. G., & Neas, L. (2013). Impact of nitrogen and climate change interactions on ambient air pollution and human health. *Biogeochemistry*, *114*(1–3), 121–134. https://doi.org/10.1007/s10533-012-9782-4
25. Piotrowicz, K., & Ciaranek, D. (2014). The impact of weather types on air pollution and health of the residents of Krakow (Poland). *2014 Air and Water Components of the Environment Conference Proceedings*, 40–47. http://aerapa.conference.ubbcluj.ro/2014/06-Piotrowicz_Ciaranek.htm. Accessed on January 14, 2022.
26. Roșu, A., Constantin, D. E., Voiculescu, M., Arseni, M., Roșu, B., Merlaud, A., Roozendael, M. Van, & Georgescu, P. L. (2021). Assessment of NO_2 Pollution Level during the COVID-19 Lockdown in a Romanian City. *International Journal of Environmental Research and Public Health 2021, Vol. 18, Page 544*, *18*(2), 544. https://doi.org/10.3390/IJERPH18020544
27. Silverman, B. W. (1986). Density Estimation for Statistics and Data Analysis - B.W. Silverman. *Monographs on Statistics and Applied Probability*. http://ned.ipac.caltech.edu/level5/March02/Silverman/Silver_contents.html. Accessed on January 9, 2022.
28. Suciu, G., Bălănescu, M., Pasat, A., Nădrag, C., Bălăceanu, C., Matei, R., Suciu, V., & Vasilescu, A. (2018). Design of a Decision Support System for Improving Air Quality Assessment. *2018 Air and Water Components of the Environment Conference Proceedings*, 221–227. https://doi.org/10.24193/AWC2018_26
29. SurveyMonkey. (n.d.). *Sample Size Calculator | SurveyMonkey*. Retrieved January 11, 2022, from https://www.surveymonkey.com/mp/sample-size-calculator/.
30. van der A., R. J., Eskes, H. J., Boersma, K. F., van Noije, T. P. C., Van Roozendael, M., De Smedt, I., Peters, D. H. M. U., & Meijer, E. W. (2008). Trends, seasonal variability and dominant NOx source derived from a ten year record of NO_2 measured from space. *Journal of Geophysical Research: Atmospheres*, *113*(D4), 4302. https://doi.org/10.1029/2007JD009021
31. Verhoelst, T., Compernolle, S., Pinardi, G., Lambert, J. C., Eskes, H. J., Eichmann, K. U., Fjæraa, A. M., Granville, J., Niemeijer, S., Cede, A., Tiefengraber, M., Hendrick, F., Pazmiño, A., Bais, A., Bazureau, A., Folkert Boersma, K., Bognar, K., Dehn, A., Donner, S., … Zehner, C. (2021). Ground-based validation of the Copernicus Sentinel-5P TROPOMI NO_2 measurements with the NDACC ZSL-DOAS, MAX-DOAS and Pandonia global networks. *Atmospheric Measurement Techniques*, *14*(1), 481–510.

https://doi.org/10.5194/amt-14-481-2021
32. Voiculescu, M., Constantin, D. E., Condurache-Bota, S., Călmuc, V., Roşu, A., & Bălănică, C. M. D. (2020). Role of Meteorological Parameters in the Diurnal and Seasonal Variation of NO_2 in a Romanian Urban Environment. *International Journal of Environmental Research and Public Health 2020, Vol. 17, Page 6228*, *17*(17), 6228. https://doi.org/10.3390/IJERPH17176228
33. World Resources Institute. (n.d.). *Global Power Plant Database*. Retrieved January 12, 2022, from https://datasets.wri.org/dataset/globalpowerplantdatabase.